Hindawi
Journal of Robotics
Volume 2024, Article ID 9896301, 1 page
https://doi.org/10.1155/2024/9896301

Retraction

Retracted: Application and Analysis of Remote Sensing Image Processing Technology in Robotic Power Inspection

Journal of Robotics

Received 23 January 2024; Accepted 23 January 2024; Published 24 January 2024

This article has been retracted by Hindawi following an investigation undertaken by the publisher [1]. This investigation has uncovered evidence of one or more of the following indicators of systematic manipulation of the publication process:

(1) Discrepancies in scope
(2) Discrepancies in the description of the research reported
(3) Discrepancies between the availability of data and the research described
(4) Inappropriate citations
(5) Incoherent, meaningless and/or irrelevant content included in the article
(6) Manipulated or compromised peer review

The presence of these indicators undermines our confidence in the integrity of the article's content and we cannot, therefore, vouch for its reliability. Please note that this notice is intended solely to alert readers that the content of this article is unreliable. We have not investigated whether authors were aware of or involved in the systematic manipulation of the publication process.

Wiley and Hindawi regrets that the usual quality checks did not identify these issues before publication and have since put additional measures in place to safeguard research integrity.

We wish to credit our own Research Integrity and Research Publishing teams and anonymous and named external researchers and research integrity experts for contributing to this investigation.

The corresponding author, as the representative of all authors, has been given the opportunity to register their agreement or disagreement to this retraction. We have kept a record of any response received.

References

[1] J. Chen, H. Yang, and R. Xu, "Application and Analysis of Remote Sensing Image Processing Technology in Robotic Power Inspection," *Journal of Robotics*, vol. 2023, Article ID 9943372, 11 pages, 2023.

Hindawi
Journal of Robotics
Volume 2023, Article ID 9943372, 11 pages
https://doi.org/10.1155/2023/9943372

Research Article

Application and Analysis of Remote Sensing Image Processing Technology in Robotic Power Inspection

Jie Chen,[1] Hemeng Yang ,[2,3] and Rui Xu[2,3]

[1]*State Grid Fujian Zhangzhou Electric Power Company, Zhangzhou, Fujian 363000, China*
[2]*China Academy of Space Technology, Beijing 100081, China*
[3]*Tianjin Zhongwei Aerospace Data System Technology Co Ltd, Tianjin 300301, China*

Correspondence should be addressed to Hemeng Yang; remotesensing@spacezw.com

Received 1 November 2022; Revised 9 December 2022; Accepted 27 March 2023; Published 15 April 2023

Academic Editor: Shahid Hussain

Along with the increase of electricity consumption in society, it means that the quality of power inspection gives higher requirements. The traditional manual inspection method is difficult to ensure the stability of checking quality. Without the popularization of manned distribution stations and smart grid methods, replacing manual inspection with electric power inspection robots can improve the inspection quality and inspection efficiency to a certain extent. Along with theimage processing process which is widely used in the robot system, visual impact is not only an effective way for us to obtain information but also the key reflection of the robot system intelligence. Unmanned aircraft as an extremely important robot has long been widely used in all walks of life. Power inspection is the most common use of unmanned aircraft robot inspection. However, due to extreme criteria such as bad weather, relative motion, and shaking of imaging equipment, inspection images are obtained ambiguously. The quality of the inspection image is related to the timely understanding, analysis, and judgment of the power engineering quality inspection database. In the paper, the unmanned aircraft power inspection robot as a scientific research foothold, according to explore the key technology of anti-internet technology to clear the image ambiguity, proposed a complete disambiguation optimization calculation method. The image denoising optimization calculation method based on the directional characteristics of time-frequency analysis and edge maintenance is selected to carry out the finding of the image, which reasonably solves the image resolution bottleneck problem of GIS in unmanned aircraft robot line inspection. Meanwhile, with the emergence of nanorobots in the 21st century, the application and analysis of remote sensing image processing technology in the field of robotic power inspection in this paper will also bring new vitality and vigor to the research of nanopower inspection robots and solve the problem of unclear images existing in nanorobots.

1. Introduction

The production and manipulation of nanorobots has been realized with the integration of robotics and information technology applications and the development of nanomaterials and technologies in manufacturing, measurement, sensors, and control systems as well as the birth of new methods [1].

The power inspection robot is a medium for the comprehensive application of power electronics, electromagnetic compatibility, image recognition, security, multisensor data fusion, big data communication, and navigation technologies in the field of substation inspection, which can discover substation equipment defects and faults in real time and at the same time can call the database for state prediction, which reduces the task of power inspection work and guarantees safe and reliable operation of the power system. In the work of electric power system, robots already have significant advantages in visual processing, distance measurement, data recording and storage, output transmission, etc., and can replace manual work with their own technical characteristics, and using robots to replace manual power inspection work can overcome the defects of manual inspection.

Drones are widely used in the daily life of the general public, and civilian-type drones are highly preferred by

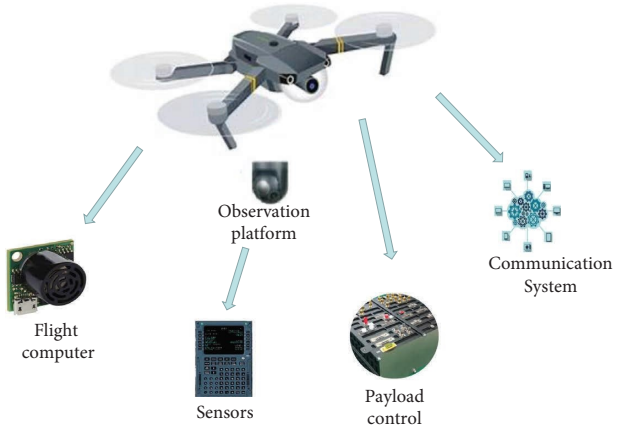

Figure 1: Structural composition of UAV remote sensing system.

young people today. UAVs are drones that can be controlled and flown by wireless remote control or by their own systems. Related industries include communication technology and information processing technology.

In the development of drones, the technicality of image processing is also important, because it can effectively distinguish the working state of the cable line. Robot system software as a contemporary high-end equipment manufacturing in the high-end equipment manufacturing is a product of the era of cross-fertilization of disciplines, with high-tech flow, high efficiency, and high socio-economic benefits of the characteristics. Drones are also the most critical kind of electric power inspection robots. Although Unmanned Aerial Vehicle (UAV) power equipment inspection technology significantly conserves both human and material resources, several pressing issues persist in its development and application process that warrant further investigation. Firstly, in the context of UAV power inspection image processing, the mobile application platform exhibits a considerable tilt angle, which is both large and irregular. This results in adjacent image navigation direction overlaps that are insufficient, with an average value of less than 20%. Moreover, the inconsistent gray values of adjacent images are detrimental to image alignment, compromising the accuracy of subsequent image processing. Secondly, the curved flight trajectory of UAVs leads to minimal horizontal overlap between adjacent images, which hinders the precise arrangement and acquisition of nodes. This issue significantly impacts the accuracy of aerial triangulation, necessitating the development of novel solutions to address these challenges in order to fully harness the potential of UAV power equipment inspection technology.. Once again, the number of images is large, the amount of data is large, and the image frames are small, and the work of piecing together the solution behind is intensive [2].

2. Theory and Methodology

2.1. Robotic Remote Sensing Technology—Take "UAV as an Example". In nanotechnology iterative upgrade in practice, intelligent robots face numerous tests, and the use of UAV aerial remote sensing for power patrol is the main filler of manned aerospace remote sensing [3]. The so-called UAV remote sensing technology refers to the combination of UAV GIS and remote sensing technology, using L-band cameras, scanners, radar detection, and other facilities, and its communication, precise measurement, and positioning technology will automatically and rapidly obtain low-altitude flight high-resolution remote sensing image data, which is an effective complement to space remote sensing and manned aerial remote sensing technology, in agriculture, forestry, land resources survey, and military. It is widely used in agriculture, forestry, land resource survey, military reconnaissance, and environmental protection.

UAV remote sensing technology can closely combine communication satellite and manned high-definition aerial photography to produce a vertical three-dimensional environmental protection monitoring service platform. The basic UAV remote sensing technology system software is mainly composed of carrier-based aircraft observation service platform, navigation electronic computer, remote sensing technology sensor, gravity gradient control board, and communication system, in which the remote sensor is shown in Figure 1, including digital cameras, scanners, radar, and other sensors.

The advantages of using UAVs for aerial remote sensing include their ability to provide fast response time, easy and reliable control, efficient data acquisition, and low cost of application [4].

2.2. Remote Sensing Image Processing Technology. Remote sensing image processing technology is the digital image processing technology that uses remote sensing technology to obtain information. The self-contained nanotechnology electronic circuit can load and process analog and digital signals and communicate with other intelligent robots external control systems. Remote sensing technology obtains information in a complicated way and must be mapping engineering and other technical ways. First of all, the earth is a sphere and must indicate the results of mapping in a plane. Because of the difference between 3D and 2D, it is possible to carry out calibration of remote sensing images directly on 2D space. The loss of the prototype of the mountains and the change of the meridian into an irregular curve map are completely unusable [5]. Thus, an efficient solution technique is important.

2.2.1. Components of Remote Sensing Image Processing Technology

(1) Indoor Spatial Resolution and Mapping Percentage. In the map production process, resolution and scale are the most important settings. On the other hand, the resolution manipulation is critically limited to the map size. Under the same specification, the larger the cut rate, the greater the precision; on the other hand, the scale of operation is also limited by the small size. Thus, when making a large HD map, the minimum specification is generally set to ensure the integrity of the scale. From the 2 specifics can learn that the limit immediately determines the level of resolution.

(2) Popper Resolution. The resolution of Popper is critically endangered by wavelength and signal frequency, and wavelength and resolution are inversely proportional. As the wavelength increases, there is an inverse relationship with resolution, resulting in diminished image quality. This phenomenon may subsequently influence the accuracy of analytical outcomes derived from the data. Typically, a shorter wavelength is preferable, as it often correlates with enhanced performance in various applications. However, there are also wavelengths restricted by the living environment. Short and medium wavelengths are difficult to obtain remote sensing technology conclusions. In order to ensure the resolution, the transmission frequency of the frequency band must have the relative density resolution.

(3) Time and Phase Difference Resolution. Remote sensing technology image processing process is applied, using the special time-length information content obtained according to the GIS and the way and method to obtain accurate images. But the image is not fixed, especially in the environment. Therefore, there are differences in the temporal resolution of the remote sensing technology conclusions in different time frames. In order to ensure the effectiveness of remote sensing technology in unique applications, it is necessary to obtain periodic transformations through long-term surveys.

2.3. Introduction of Electric Power Inspection Robots

2.3.1. Types of Power Inspection Robots. Nanorobots as a kind of functional special tool different from the past have shown strong power in all walks of life [6]. Power inspection robots as a key kind of robots, according to the basic elements and integration into the place, can be divided into in-room inspection robots, outdoor inspection robots, tunnel construction inspection robots, and unmanned aircraft inspection robots. It is divided into crawler, wheel test, and crawler based on the posture type.

(1) Electric tunnel construction track inspection robot is used for electric tunnel construction environment, such as comprehensive electric underground corridor. Electric power tunnel construction necessitates the assembly of a stationary, fixed track system. A patrol robot traverses this track, inspecting areas designated for the installation of fixed, immobile tracks.

(2) Outdoor crawler patrol robot for outdoor environment, such as outdoor column power switch and substation transformer area, has no requirement for the road environment, according to the navigation and positioning system to carry out inspections in the set area.

(3) Unmanned aerial inspection robots, designed for high-voltage transmission lines and other elevated environments, employ navigation and positioning systems within designated channel areas to conduct safety inspections effectively and accurately.

2.3.2. UAV Robot Power Inspection. Along with the development of intelligent robotics, robots with very different roles play an increasingly important role in human daily life and industrialized production, becoming the right-hand man. The application range of robotic technology extends from the depths of the ocean floor to terrestrial environments and into the vast expanse of outer space, facilitating human exploration of an increasingly expansive realm. Among them, the application of robots in power inspection is also becoming more and more extensive.

Traditional power inspection relies on human resources, and in order to ensure the normal operation of the supply and distribution system, regular inspection and maintenance of the Koran voltage power system such as tower poles, power lines, and composite insulators in power lines are carried out according to the on-site survey of power workers. On the other hand, in remote mountainous areas, inspectors can use binoculars to view and check the distant areas or climb to the tower base in mountainous areas to carry out inspections which is restricted by the accumulated experience of people of all shapes and sizes and the extreme terrain of remote areas. This type of inspection is not efficient, and labor efficiency, low safety factor, and some visually blind areas cannot be inspected [7]. The occurrence of drone inspection technology can well prevent the dangers and shortcomings of manual inspection. Contemporary drone reconnaissance is a new type of reconnaissance technicality that combines drones closely with infrared thermal imager, remote sensing technology, surveillance camera machines, and equipment to carry out reconnaissance daily tasks in certain scenes which is widely used in all walks of life.

At this stage, the power inspection industry is the most common use of drones in the industry. In contrast to manual power inspection methods, drone technology offers superior capabilities, such as vertical descent at any given moment and a high degree of precision in navigation. These features enable the execution of inspections at any time and location along the designated route. Furthermore, the drone's perspective can be adjusted as needed to ensure a comprehensive examination of the power inspection route, adhering to established guidelines. The drone has intelligent control technology, which can remotely control and adjust the aircraft flight height, target, and course according to the inspection regulations, with high fault tolerance.

2.4. Image Denoising Algorithm. During the utilization of Unmanned Aerial Vehicle (UAV) robots for power inspection processes, including power station monitoring, line imagery, and image transmission, the presence of signal interference may introduce Gaussian noise into the captured images. This phenomenon not only disrupts the UAV's normal flight but also significantly impacts the imaging quality of the inspected circuitry.

2.4.1. Noise Source and Model. Noise is one of the key factors in controlling image resolution. There are three key sources of image noise. First, the Gaussian function noise caused by

arbitrary thermal motion of electrons during the operation of the component is generally indicated by the zero-mean, Gaussian function white noise with stable compressive strength scattering. Second, the optical lens photoelectric conversion link by the influence of light Poisson noise is particularly weak, often indicated by a Poisson density distribution of random variables [8]. Third, the particle noise generated in the optical induction in the image is generally indicated by Gaussian function noise. Gaussian function noise is the most common and important noise with a probability density function of

$$p(z) = \frac{1}{\sqrt{2\pi}\sigma} \exp\left[\frac{-(z-\mu)^2}{2\sigma^2}\right], \quad (1)$$

where z indicates the gray level and relative standard deviation of the sharpness of the image. When z follows the above equation throughout, 70% of the values fall in the range $[(\mu - \sigma), (\mu + \sigma)]$, 95% fall in the range $[(\mu—2\sigma), (\mu + 2\sigma)]$, and 99.7% fall in the range $[(\mu - 3\sigma), (\mu + 3\sigma)]$.

2.4.2. Basic Principle of Wavelet Transform Denoising. Wavelet transform is a new way of transform analysis. It inherits and cultivates the concept of localization of short-time Fourier transform and at the same time solves the defect that the window size does not follow the change of frequency. It is an ideal tool for analyzing and processing the signal-duration-frequency by providing a "duration-frequency" dialog box with frequency. The wavelet optimization algorithm can decompose the complex filtering process into many simple processes, each of which is reversible. The wavelet transform maintains the concept of excellent localization of short-time Fourier transform, while solving the defect that the window size does not follow the frequency change, bringing the time-frequency dialog box with frequency change. The subband signal obtained by the decomposition has multiresolution, dual-frequency, and multidirectional characteristics, called optical microscopy [9]. The main advantages are low entropy, multiresolution, selective substrate picking coordination capability.

(1) Continuous Wavelet Transform. Let $\psi(t)$ be a square can accumulate function formula function whose Fourier transform has $\omega = 0$ at $\psi(0) = 0$, i.e., $\int_{-\infty}^{\infty} \psi(t)dt = 0$, then $\psi(t)$ is said to be the fundamental wavelet or mother wavelet [10]. The mother function formula is deflated to become:

$$\psi_{a,b}(t) = \frac{1}{\sqrt{|a|}} \psi\left(\frac{t-b}{a}\right), a, b \in R, a \neq 0, \quad (2)$$

in which $\psi_{a,b}(t)$ is referred to as the wavelet function formula. Here, the average error or total width of the wavelet function represented by the independent variable a is called the scale factor, and the spacing of the independent variable b moving in the t-axis is called the translation factor. The energy of the mother wavelet $\psi(t)$ is concentrated at the

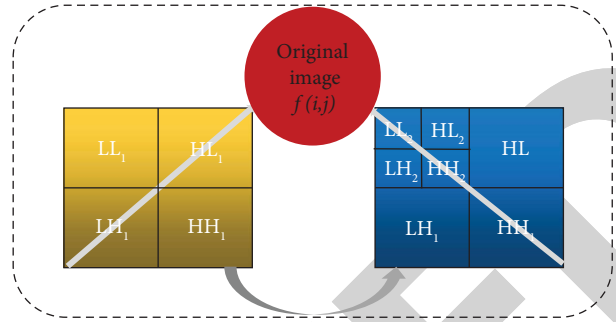

Figure 2: Wavelet decomposition schematic.

starting point, and the kinetic energy of the wavelet function $\psi_{a,b}(t)$ is concentrated at point b.

The formula for the continuous wavelet transformation of the arbitrary function is shown as follows:

$$W_f(a,b) = \langle f, \psi_{a,b} \rangle = \frac{1}{\sqrt{|a|}} \int f(t) \psi * \left(\frac{t-b}{a}\right) dt, \quad (3)$$

in which $\psi * (t)$ is expressed as the complex conjugate point of $\psi(t)$.

When the wavelets are orthogonal, the reconstructed formula according to the wavelet inverse transform is

$$f(t) = \frac{1}{C_\psi} \int_{-\infty}^{\infty} \int_{-\infty}^{\infty} \frac{1}{a^2} W_f(a,b) \psi\left(\frac{t-b}{a}\right) dadb. \quad (4)$$

(2) Discrete Wavelet Transformation. In the majority of computer implementations, discrete wavelet transforms are employed. The primary parameters, including the scaling factor and the translation factor, are derived from the discrete wavelet transform process.

Generally, we use the method of continuous wavelet conversion parameter discretization formula for $a = 2^{-j}$ and move the main parameters for $b = k2^{-j}$, where $k, j \in Z$. The formula for wavelet conversion $\psi_{j,k}(t)$ is shown as follows:

$$\psi_{j,k}(t) = 2^{j/2} \psi\left(\frac{t - k2^{-j}}{2^{-j}}\right) = 2^{j/2} \psi\left(2^{-j}t - k\right). \quad (5)$$

Discrete wavelet transformation index is shown as follows:

$$C_{j,k} = \langle f, \psi_{j,k} \rangle = \int_{-\infty}^{\infty} f(t) \psi_{j,k}(t) dt. \quad (6)$$

The reconstructed formula is shown as follows:

$$f(t) = C \sum_{-\infty}^{\infty} \sum_{-\infty}^{\infty} C_{j,k} \psi_{j,k}(t). \quad (7)$$

C is a constant that is not associated with the data signal. The power precision of the signal can be reconstructed according to picking the best j and k.

After discrete quadrature and wavelet transformations, as shown in Figure 2, each image is decomposed into four subimages. The top left is originally a smooth analog of the image, called the low frequency LL subimage, and the rest of

the image is originally a small detail of the image, with high frequency information content. The lower left has small details of vertical edges with high frequency LH subimages, the upper right has small details of level edges with high frequency HL subimages, and the lower right has small details of diagonal edges with high frequency HH subimages. We have 3N high frequency bands and 1 low frequency band for different types of (3N-1) body height images when we carry out nth-order wavelet dissolution for 2D images. Due to uneven sunlight, dust, and other relatively complex natural environment, the UAV power inspection robot vision recognition system to extract images, there is a certain amount of noise. Employing wavelet optimization algorithms for rapid denoising can conserve computational memory, thereby enhancing the overall performance of inspection robots' visual navigation systems.

2.5. Defuzzification Loss Function. Due to the weather and instability of the airframe and other reasons, the UAV power inspection recognition images have the problem of blurring. And with the wide application of remote sensing image processing technology in the field of nanorobot research, the research related to blurred image recovery has become increasingly mature. This study takes the deblurring loss function as the starting point to solve the blurring problem of robotic power inspection images.

2.5.1. Content Loss Function. The content missing function is a computational function formula used to measure the difference between the estimated value of the model $f(x)$ and the middle of the true value y. This is the nonnegative real-valued function formula, which is generally indicated by $L(Y, f(x))$. The lower the loss function is, the better the robustness of the model is. Content loss is used to accurately measure the content similarity between the generated instance image and the actual instance image [11]. The concept of image content is very general and contains multisensor fusion, pixel content, image construction, and gradient orientation. In this paper, the constraints on the generated images are carried out in terms of both pixel content and image spatial features to ensure the consistency in content between the generated reconstructed images and the real clear images, which is the core of the remote sensing image processing technique in this paper and provides a solution to the image blurring problem in robotic power inspection.

(1) Pixel Deviation Constraint. Among the loss functions constrained according to pixel deviation, $L1$ loss and $L2$ loss are commonly used. $L1$ depletion and $L2$ loss are also known as mean relative error (MAE) and root mean square error (MSE). They are able to measure the mean value of the distance $L1$-$L2$ of the corresponding pixel points between the generated sample plate image and the actual sample plate image.

In the image super-resolution reconstruction and blur removal approach, $L2$ loss of key is used as content loss. The image quality is reconstructed based on the $L2$ spacing between the pixel values of the two images reduced to the minimum. However, because of the $L2$ spacing self-design problem, the reconstructed image becomes smoother, and blurring in the image details is inevitable. In the paper, LI damage is selected as the pixel deviation constraint of the model. The calculation formula is shown as follows:

$$L_{\text{pix}} = \frac{1}{WH} \sum_{x=1}^{W} \sum_{y=1}^{H} \left| I_s - G_{\theta_G}(I_B)_{x,y} \right|, \tag{8}$$

in this context, W and H represent the dimensions and overall width of the sample image, respectively. Here, this is also the generated image that is specific to the image. Depending on the bounded LI spacing, the consistency of the generated image with the actual image's middle pixel content can be ensured.

(2) Spatial Feature Tubing. With the rapid development of science and technology, the generation, fabrication, and development of nanomaterials in the UAV robotic power inspection technology gradually formed a good possibility; however, robotic power inspection technology faces with the problem of unclear images of the inspection system, and pixel-level deviation ensures the similarity of the content of two images clarity but ignores the cognitive differences between the images [12]. Therefore, by acquiring the feature maps of each convolutional layer keyed to the image in the special network model, the $L2$ spacing between the feature maps of the formed image and the real image is improved according to limiting the high-frequency information content of the formed image and leaving more image key points. However, the network model of the convolutional layer must be available to measure the feature cognitive damage of the image [13]. Here, the VGG Internet is used as an example, and the flow of the measurement procedure is shown in Algorithm 1.

The equation of the geospatial elements governing the relationship in the entity model is shown as follows:

$$L_{\text{feat}} = \frac{1}{W_{i,j} H_{i,j}} \sum_{x=1}^{W_{i,j}} \sum_{y=1}^{H_{i,j}} \left(\phi_{i,j}(I_S)_{x,y} - \phi_{i,j}\left(G_{\theta_G}(I_B)\right)_{x,y} \right)^2. \tag{9}$$

In the given context, the terms refer to the subspaces of feature images prior to the jth convolutional layer and subsequent to the Ith max-pooling layer within the VGG19 network architecture, respectively. The calculation steps of the specific feature-aware deficit are shown in Figure 3. The perceptual damage of the formed image in the convolutional layer Conv3_2 and the feature map of the actual image are measured on the figure using the VGG19 Internet as an example.

3. Solution Measures

3.1. Image Denoising Optimization Algorithm Based on Wavelet Transform Directional Characteristics and Edge Maintenance

3.1.1. Directional Characteristics of Wavelet Transform. After wavelet transform dissolution, the low frequency component of the image is very similar to the original image,

Input: Generate sample Im_1 and real sample Im_2
(1) Initialize the trained VGG network based on the sample images
(2) Feature extraction of input sample images using VGG
(3) For $m = 1, 2, \ldots, n$ do
(4) Calculate the $L2$ distance of the corresponding feature map of the image to be measured
(5) For $m = 1, 2, \ldots, n$ do
(6) End
Output: Perceptual loss of the two images

Algorithm 1: Perceived Loss Calculation Process.

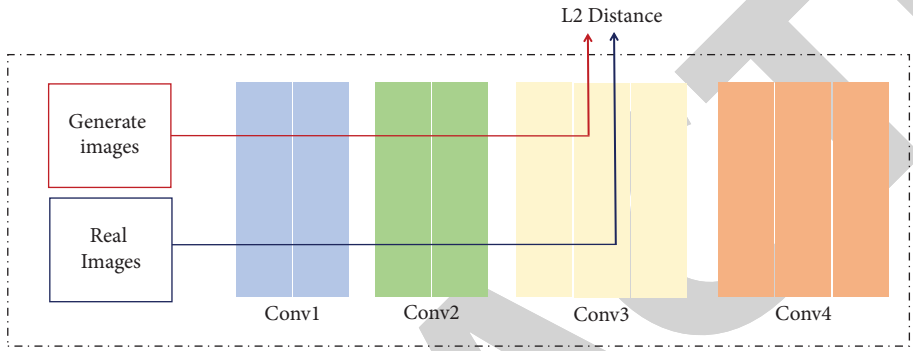

Figure 3: Feature perception loss calculation.

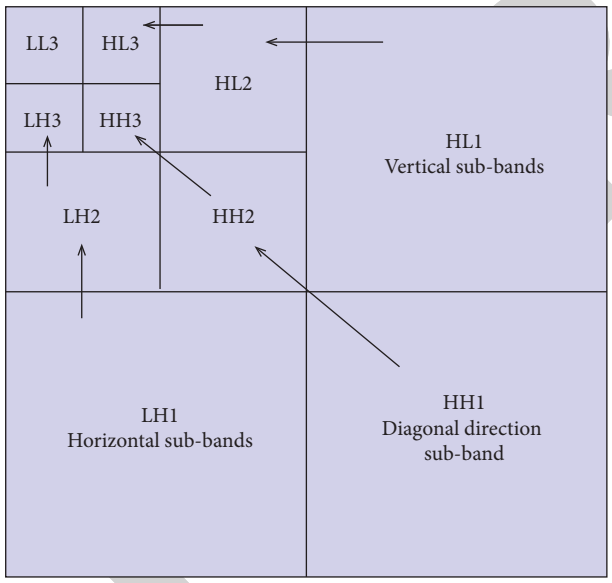

Figure 4: Wavelet decomposition high frequency subband directional characteristics.

but the high frequency component converges the important kinetic energy of the original image and exhibits the characteristics of the original image transformation such as edges [14]. In addition, most of the noise is also present in this component; thus, there is a great need to remove the high frequency component noise. As shown in Figure 4, the triple wavelet transform construction diagram shows the low frequency components of the original image, and HL1, HL2, and the three dissolved scales of the original image in the vertical direction of the edges and details. As well, LH, LH2, HH2, and HH each indicate the data in the horizontal and diagonal directions.

3.1.2. Algorithm Flow. Drive technology is one of the important components of the scholarly study of microstructure intelligent robots. Different types of drive forms not only have a great impact on the speed and form of motion of micro and nanorobots and limit the application scenarios of micro and nanorobots [15]. The process of robotic power inspection applications involves the drive technology of the controller, and this paper uses wavelet conversion directional characteristics and edge-maintained image denoising algorithms to design unique algorithmic processes for the development of nanorobot drive technology. The steps are summarized in Figure 5.

(1) We perform wavelet dissolution on images with Gaussian white noise primaries.
(2) We perform filtering of the high frequency orientation subgraph to remove noise based on the SVD decomposition of the orientation characteristics and reconstruct the number of singular values determined by the response equation of the elasticity coefficient of the highest value frequency stability. On the other hand, the edges of each subgraph are obtained using the azimuthal edge checking algorithm.

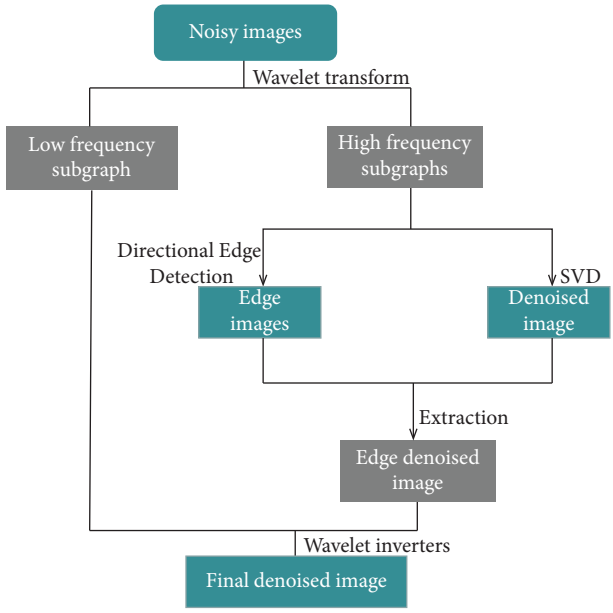

Figure 5: Image denoising algorithm flow.

3.2. Optimization Algorithm for Power Generation Cast Power Safety Inspection Deambiguation According to RRDB

3.2.1. The Imaging Stage Model of Intelligent Robot Power Safety Inspection—Taking UAV as an Example. Intelligent monitoring robot development has the characteristics of manipulation and operation mode dexterity and will not be affected by temperature factors. In unmanned or unmanned distribution stations, substations repeatedly implement inspection daily tasks. Unmanned Aerial Vehicle (UAV) technology facilitates power safety inspections by acquiring imagery of power infrastructure, enabling technicians to perform routine examinations and analyses of electrical circuits more efficiently. From the perspective of electro-optical imaging, a process of UAV reconnaissance image acquisition is to reconnoitre the target radiation source keyed to the load module output electro-optical stage. However, the full imaging process includes not only electro-optical imaging but also the main parameters used to specify the imaging quality with a daily task model corresponding to the daily task of the specific loop system [16]. The full process of UAV robotic power inspection imaging can be understood as a reconnaissance imaging stage model consisting of imaging model, main parameter model, and daily task model. The small details of the model are shown in Figure 6.

(1) Inspection task model: According to the specific inspection system daily task requirements, the relevant evaluation index system is applied to clarify the daily task evaluation index system. Before oil and gas well inspection, the planned task should be developed, including inspection line, inspection task, and main parameter setting.

(2) Main parameter model: The main parameter model is created according to the gimbal attitude shift, the main parameters of the surveillance camera image, geomorphology, pathways, and other environmental elements in the mission planning. It brings an important guarantee for the successful completion of the UAV inspection.

In the above UAV reconnaissance image linking model, the sensing device transmits the visible light band of the photographed image. However, the entire transmission process suffers from the inherent characteristics of the machine and equipment and the influence generated by electromagnetic interference, which also generates inevitable random noise, and the quality of the collected inspection images will be reduced. In addition, the UAV in the navigation link, the shaking of the gimbal, attitude shift, and relativity calibration transport will cause the image bias position, resulting in circular system image motion blur. Thus, there are more than 2 causes of UAV reconnaissance image recession: random noise and motion blur caused by poor fitness movement during imaging.

3.2.2. Construction of Power Patrol Dataset. Drones and nanorobots can cause blurred recognition images during power inspections due to weather, vibration, and other reasons. The image defuzzification daily task is used to perform defuzzification on a dataset in order to train and test the model's defuzzification level. A common blurred clearing dataset is a pair of images that must be "blurred-dynamically blurred". In paired datasets, the blurred and clear images should be one-to-one in terms of content and structure. Obtaining the appropriate "blurred-clear" image pairs is not a simple daily task.

The basic principles of image degradation were used to simulate the motion blur generated by the unmanned aircraft during the process of image development, resulting in an electronic reconnaissance blurred image. The motion blur process is generally a linear degradation process, and the degraded entity model can be defined as follows:

$$g(x, y) = \oint(x, y) * h(x, y) + n(x, y), \tag{10}$$

in which $h(x, y)$ is the space of degradation function indicates that the convolution sum is degraded blurred image and clear image. In the specific image process, the effect of random noise is inevitable.

The change in direction and speed of the UAV robot after implementing the electric power engineering inspection task depends on the direction and level of the motion blur [17]. The point spread function formulation has two extremely important main parameters: the fuzzy direction and the fuzzy scale. The direction of blurring needs to be indicated by the angle between the direction of motion and the horizontal direction, and the blurring limit can control the level of the degraded image. Different types of blurring main parameters can mix different directions and levels of motion blurred images. Thus, in this paper, the point spread function formula is used to create a "blurred-clear" image pair for the robotic power inspection. Then, to

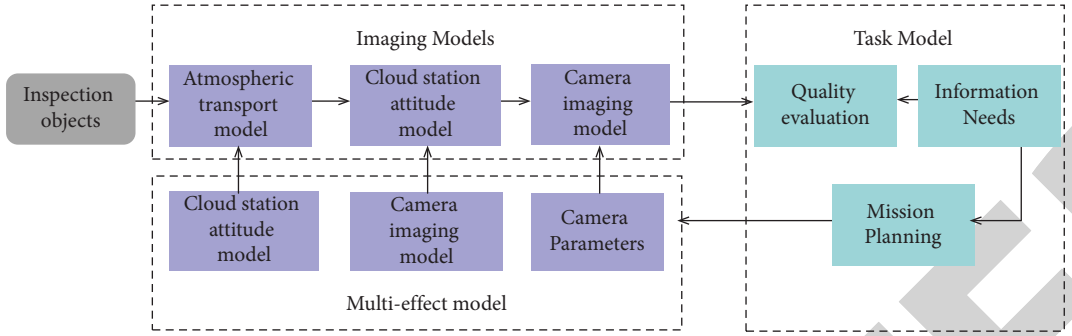

Figure 6: UAV inspection imaging link model.

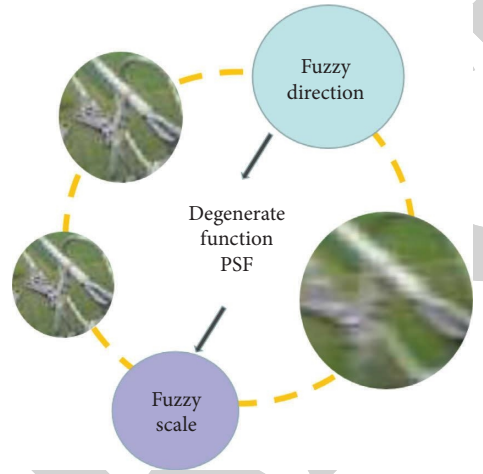

Figure 7: Motion blur patrol image synthesis.

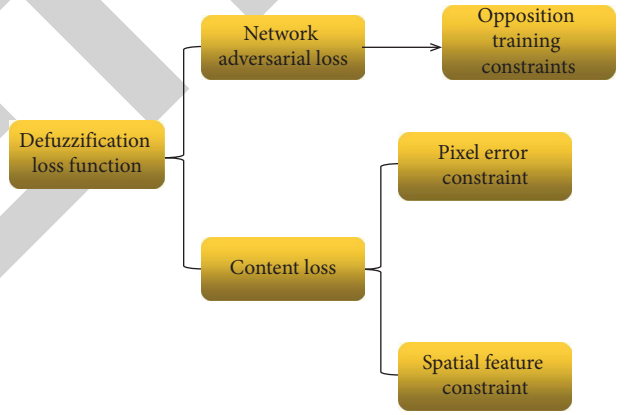

Figure 8: Overall design of the deblurring model.

ensure the diversity of the generated fuzzy inspection image samples, different types of fuzzy main parameters are set. Eventually, the prepared processed circulatory system image is keyed in, and the blurred unclear degradation solution is carried out using the degradation function formula PSF to generate the motion blurred system image corresponding to the clear circulatory system image. The full process of generation is shown in Figure 7.

3.2.3. Overall Scheme Design of Fuzzy Loss Function Formulation. The output language of the fuzzy controller expresses the independent variables selected as easy as possible, and taking into account the specific situation of intelligent robot walking and obstacle avoidance, the range sensor and direction sensor are selected to be able to better integrate into the whole process of robot obstacle avoidance. The collected information content of external factors is made

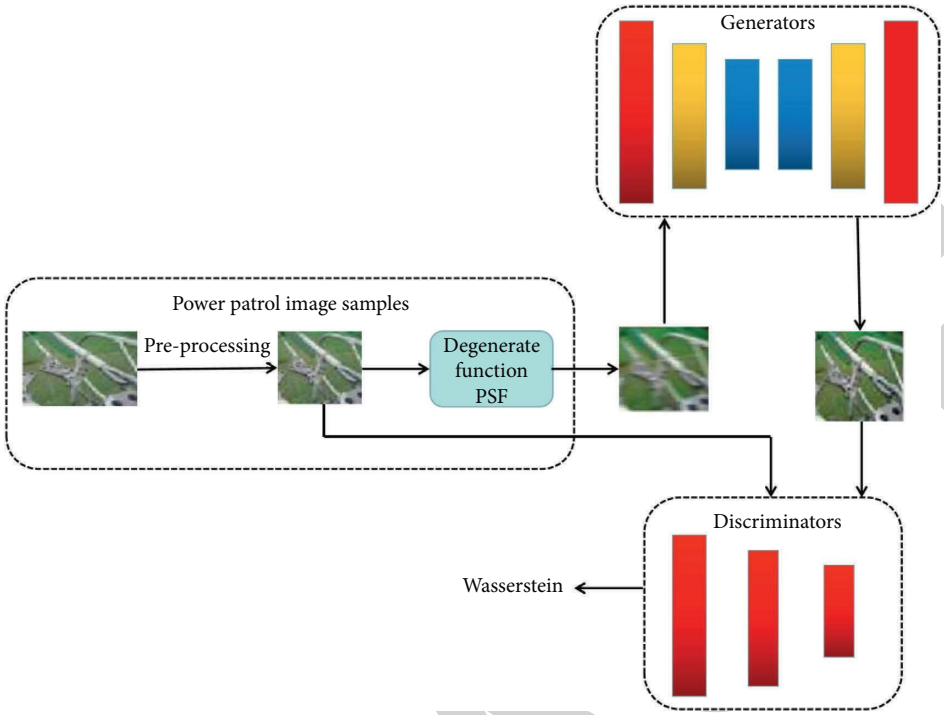

Figure 9: Overall process of deblurring power inspection image.

as the key to the fuzzy controller, the damage of the fuzzy controller is made as the robot target control, and the core of fuzzy controller is the establishment of fuzzy loss function [18].

The loss function formulation of the fuzzy unclear model contains two categories of Internet adversarial loss and content loss. Confrontation loss practices the maker and classification algorithm confrontation according to a very small notion of gaming [19]. Specific content loss means that the produced image information is managed to form a high-quality deblurred image based on the clarity deviation and spatial characteristics of the image. The integrated design of the ambiguity removal model is shown in Figure 8.

The coefficients of the three loss functions are computed, representing the loss functions of the ambiguity model discussed in the text. The expressions for these functions are as follows:

$$L = L_{\text{adv}} + \lambda_1 L_{\text{pix}} + \lambda_2 L_{\text{feat}} \tag{11}$$

3.3. Electricity Inspection Image Deblurring Process. For the image blurring problem in the power inspection of the UAV robot, the fuzzy entity model of the power generation grid-connected power inspection according to the RRDB network unit is developed, and the repair and reconstruction of the blurred inspection image are completed. The blurred processing of the switching power check image is shown in Figure 9.

A process of power inspection wild blur simulation can be summarized as follows: the first use of image recession model to simulate the blurred inspection images is generated during the robot inspection, and then, the "blurred and clear" power inspection image pairs are each keyed into the generator and classification algorithm in the entity model. Under the practice of the generator and classification algorithm, the generator maintains the image formation level and finally forms a replica image that is highly consistent with the clear power electronic reconnaissance image sample. The whole process is completed with a UAV representing the actual operation of robotic power inspection image deblurring [20]. At present, the development of nanomaterial robots in industries such as natural environment exploration, cosmic exploration, and power inspection is still in the preliminary stage, and the above-mentioned deblurring process to solve the image blurring problem can recommend its further commercialization.

4. Conclusion

At the present stage, the panoramic image imaging technology based on image stitching within the UAV panoramic image remote sensing technology system has many problems such as relatively slow development speed, poor practicality, difficulty in obtaining dynamic and complete panoramic images, large amount of image data obtained, and complicated stitching optimization algorithm. According to the exploration of the UAV remote sensing

technology instant panoramic imaging technology and remote sensing technology, image processing process, for this subject research, has practicality, wide line of sight, strong manipulation, low cost, and relatively loose operating standards, and good image visual quality of remote sensing images can also establish the technical strength of the current stage of UAV robotic power inspection and promote the full effectiveness of the UAV monitoring system.

The key in the paper explores the UAV instant panoramic image GIS as well as the image processing process. The test results show that the denoising optimization algorithm proposed in the paper is useful to preserve small details of Kor-voltage towers, power lines, and Kor-voltage hardware configurations, giving effective application for safety risk evaluation in the electric power industry. In the future, the use of remote sensing technology image processing process in robotic power inspection will become more and more critical. The visual recognition system of nanocomposite robots has the advantages of noncontact, relatively high dexterity, rich content, and visualization of figurative data, which also gives higher technical performance to the software of high precision visual effect sensor system, and it is believed that the remote sensing image processing technology will also be applied to the manufacturing and research of nanocomposite robots in the future [21].

Data Availability

The labeled data used to support the findings of this study are available from the corresponding author upon request.

Conflicts of Interest

The authors declare that there are no conflicts of interest.

Acknowledgments

This work was supported by the Science and Technology Project of State Grid Fujian Electric Power Company (Research on Risk Prediction Technology of Transmission Channel Tree Obstacle based on UAV LiDAR, No. 52135020000N).

References

[1] A. Benouhiba, L. Wurtz, J. Rauch, J. Agnus, K. Rabenorosoa, and C. Clévy, "Nanorobotic structures with embedded actuation via ion induced folding," *Advanced Materials*, vol. 33, no. 45, Article ID 2103371, 2021.

[2] W. Wang, X. Yu, B. Fang et al., "Cross-modality LGE-CMR segmentation using image-to-image translation based data augmentation," *IEEE/ACM Transactions on Computational Biology and Bioinformatics*, vol. 1, 2022.

[3] A. B. Alhassan, X. Zhang, H. Shen, H. Xu, K. Hamza, and G. Masengo, "Precise motion control of a power line inspection robot using hybrid time delay and state feedback control," *Frontiers in Robotics and AI*, vol. 9, Article ID 746991, 2022.

[4] D. Salley, G. Keenan, J. Grizou, A. Sharma, S. Martín, and L. Cronin, "A nanomaterials discovery robot for the Darwinian evolution of shape programmable gold nanoparticles," *Nature Communications*, vol. 11, no. 1, p. 2771, 2020.

[5] A. Tiwari, S. K. Sharma, A. Dixit, and V. Mishra, "UAV remote sensing for campus monitoring: a comparative evaluation of nearest neighbor and rule-based classification," *Journal of the Indian Society of Remote Sensing*, vol. 49, no. 3, pp. 527–539, 2020.

[6] S. Ghaffarian, J. Valente, M. van der Voort, and B. Tekinerdogan, "Effect of attention mechanism in deep learning-based remote sensing image processing: a systematic literature review," *Remote Sensing*, vol. 13, no. 15, p. 2965, 2021.

[7] N. Guan and P. Zhang, "Active compliance control system for intelligent inspection robot in power room," *Journal of Control Science and Engineering*, vol. 2022, Article ID 7829082, 7 pages, 2022.

[8] T. Wang, K. Fang, W. Wei, J. Tian, Y. Pan, and J. Li, "Microcontroller unit chip temperature fingerprint informed machine learning for IIoT intrusion detection," *IEEE Transactions on Industrial Informatics*, vol. 19, no. 2, pp. 2219–2227, 2023.

[9] D. Dhongade and M. Patil, "EEG based brain computer interfacing for hand assistant system using wavelet transform," *ITM Web of Conferences*, vol. 32, p. 03035, 2020.

[10] H. Rao, S. Wang, X. Hu et al., "A self-supervised gait encoding approach with locality-awareness for 3D skeleton based person Re-identification," *IEEE Transactions on Pattern Analysis and Machine Intelligence*, vol. 1, 2021.

[11] S. Kesornprom, P. Cholamjiak, and C. Park, "New proximal type algorithms for convex minimization and its application to image deblurring," *Computational and Applied Mathematics*, vol. 41, no. 7, p. 333, 2022.

[12] G. Rigatos, N. Zervos, P. Siano, M. Abbaszadeh, J. Pomares, and P. Wira, "A nonlinear optimal control approach for underactuated power-line inspection robots," *Robotica*, vol. 40, no. 6, pp. 1979–2009, 2022.

[13] W. Xiong, S. Yang, Z. Zhang, L. Chen, and S. Huang, "Research on image recognition of power inspection robot based on improved YOLOv3 model," *Journal of Physics: Conference Series*, vol. 1486, no. 4, Article ID 042034, 2020.

[14] D. K. Alves, R. L. A. Ribeiro, L. F. D. Q. Silveira, and T. O. A. Rocha, "Real-timewavelet-based adaptive algorithm for low inertia AC microgrids power measurements," *International Journal of Electrical Power & Energy Systems*, vol. 140, Article ID 108043, 2022.

[15] T. Wang, B. Lu, W. Wang, W. Wei, X. Yuan, and J. Li, "Reinforcement learning-based optimization for mobile edge computing scheduling game," *IEEE Transactions on Emerging Topics in Computational Intelligence*, vol. 7, no. 1, pp. 55–64, 2023.

[16] C. Wang, Z. Li, Y. Kang, and Y. Li, "Applying SLAM algorithm based on nonlinear optimized monocular vision and IMU in the positioning method of power inspection robot in complex environment," *Mathematical Problems in Engineering*, vol. 2022, Article ID 3378163, 14 pages, 2022.

[17] T. Wang, J. Li, W. Wei, W. Wang, and K. Fang, "Deep-learning-based weak electromagnetic intrusion detection method for zero touch networks on industrial IoT," *IEEE Network*, vol. 36, no. 6, pp. 236–242, 2022.

[18] Y. Kim, J. K. Chae, J. H. Lee, E. Choi, Y. K. Lee, and J. Song, "Free manipulation system for nanorobot cluster based on complicated multi-coil electromagnetic actuator," *Scientific Reports*, vol. 11, no. 1, p. 19756, 2021.

[19] W. Shao, Z. You, L. Liang et al., "A multi-modal gait analysis-based detection system of the risk of depression," *IEEE Journal of Biomedical and Health Informatics (JBHI)*, vol. 26, no. 10, pp. 4859–4868, 2022.

[20] X. Xu, K. Watanabe, and I. Nagai, "Flight control system design for a tandem rotor UAV robot in the presence of wind field disturbances," *Artificial Life and Robotics*, vol. 26, no. 4, pp. 457–464, 2021.

[21] M. Suhail, A. Khan, M. A. Rahim et al., "Micro and nanorobot-based drug delivery: an overview," *Journal of Drug Targeting*, vol. 30, no. 4, pp. 349–358, 2021.